Physicochem. Probl. Miner. Process. 53(1), 2017, 264−278

www.minproc.pwr.wroc.pl/journal/

Physicochemical Problems of Mineral Processing

ISSN 1643-1049 (print)
ISSN 2084-4735 (online)

Received April 4, 2016; reviewed; accepted June 27, 2016

ADSORPTION BEHAVIOR OF Zn(II) ONTO NATURAL MINERALS IN WASTEWATER. A COMPARATIVE STUDY OF BENTONITE AND KAOLINITE

Wencui CHAI, Yanfang HUANG, Shengpeng SU, Guihong HAN, Jiongtian LIU, Yijun CAO

School of Chemical Engineering and Energy, Zhengzhou University, Zhengzhou, P.R. China, guihong-han@hotmail.com

Abstract: In order to remove the harmful metal ions in lead-zinc mineral processing wastewater, two natural clay minerals (bentonite and kaolin) were used as adsorbents and Zn(II) ions were the emphasis in this work. The adsorption behaviors including kinetics and isotherms were investigated by batch experiments. In addition, the adsorption mechanisms were studied by means of zeta potential testing, optical microscope and XRD analysis. The results show that the adsorption process can be best described as the pseudo-second order kinetic model. The adsorption equilibrium data of bentonite and kaolinite can be respectively fitted best by Langmuir and Freundlich models. Thermodynamic studies display that the adsorption of Zn(II) onto clays is non-spontaneous and endothermic. The maximum capacity of Zn(II) adsorbed on bentonite and kaolinite respectively reaches to 79.2 $mg \cdot g^{-1}$ and 6.35 $mg \cdot g^{-1}$ at 25 °C. The structural differences of bentonite and kaolinite result in the differences in adsorption behavior and mechanism. The interaction mechanisms of Zn(II) with bentonite and kaolinite involve electrostatic attraction, cation exchange, surface complex and precipitation. Bentonite as adsorbent has the potential to remove Zn^{2+} better than kaolinite.

Keywords: *adsorption, Zn(II), wastewater, clay minerals, structural properties*

Introduction

With the development of mining industry, a large amount of heavy metals such as lead, zinc and copper have been released into the environment and have polluted water resources, soils and crops. The pollution of lead-zinc mineral processing wastewater has been aroused a special concern in China, since China is one of the largest producers and consumers of lead and zinc in the world (Zhang et al., 2012). Therefore, wastewater treatment and cycle-use have much academic and practical significance for the environmental protection and water conservation.

http://dx.doi.org/10.5277/ppmp170122

Lead-zinc mineral processing wastewater mainly contains lead and zinc ions, suspended solid particles and some chemicals (Chen et al., 2009). There are many treatment techniques including coagulation precipitation, electrochemical treatment, ion flotation, adsorption, membrane technology and so on (Chen et al., 2009; Mavrov et al., 2006; Nunez et al., 2011; Polat et al., 2007; Singanan, 2011, Huang et al., 2016). Among these techniques, adsorption has been proved to be an effective and economic method for heavy metal wastewater treatment in terms of flexible operation, high adsorption capacity and easily accessible adsorbents (Fu et al., 2011; Jiang et al., 2010; Lollino et al., 2015; Melichova et al., 2013; Mohan et al., 2006; Srivastava et al., 2005; Wang et al., 2010).

Clay minerals are one of good adsorbent alternatives because of their large surface areas, high ion exchange capacities, layered structure and chemical/mechanical stability. Bentonite and kaolinite are two natural and common aluminosilicate clay minerals with smectitic structures. These two clays hold a permanent negative charge, $\equiv X^-$ on the basal surfaces, and a smaller variable charge, ≡SiOH on the mineral edges (Gu et al., 2008; Gu et al., 2010), which could provide plentiful adsorption sites for metal ions. There have been some studies using natural clays mainly bentonite and kaolinite to remove Zn(II) from aqueous solution (Dukic et al., 2015; Musso et al., 2014). The adsorption of Zn(II) onto natural bentonite and acid washed-kaolinite at acidic and neutral environment was reported (Sen et al., 2011; Arias et al., 2009). The results showed that the adsorption process followed pseudo-second-order kinetic model and the equilibrium adsorption was fitted better with Langmuir isotherm. Srivastava et al. (2005) investigated the adsorption behavior of Zn(II) with very low concentration (<8.66 $mg \cdot dm^{-3}$) onto kaolinite. The results showed that ion exchange reaction occurred at pH<7.0 and inner-sphere surface complexes were prone to form at higher pH. However, similar studies were mainly focused on the influencing factors, kinetics and adsorption isotherms, without considering the difference in the clay structures and their properties (Mellah et al., 1997; Bereket et al., 1997; Sheta et al., 2003; Kaya et al., 2005; Veli et al., 2007; Kubilay et al., 2007). Therefore, the effects of clay structures and properties on adsorption process need to be further studied.

In this work, two natural silicate clay minerals, bentonite and kaolinite were used as Zn(II) adsorbents to evaluate their adsorption behaviors. The factors influencing the adsorption process, kinetics, isotherms and thermodynamics were investigated. What is important is that, the difference in adsorption mechanisms between two clays was inspected using advanced analysis techniques including optical microscope, scanning electron micrographs, X-ray diffraction and microscopic electrophoresis analysis.

Experimental

Materials

The bentonite (montmorillonite content of 95.8%) was obtained from a mineral processing plant in India. The kaolinite (analytical grade) was purchased from Tianjin

Chemical Reagent Technologies Co., Ltd, China. Both clay samples were further dried at 105 °C for 24 h. The specific surface areas of two clay samples were measured using a surface area tester (NOVA ST-2000, America) and calculated by the BJH method. The specific surface area of bentonite and kaolinite is 17.767 $m^2 \cdot g^{-1}$ and 10.562 $m^2 \cdot g^{-1}$ respectively. The equilibrium pH method was used to determine and calculate CEC values for the two clays (Jackson, 1962; Aprile et al., 2012). The CEC of bentonite and kaolinite is respectively 86.4 and 13.5 meq/100 g clay.

Unless specifically noted, all reagents used in the experiments were analytical grade and were used without further purification. A 1000 $mg \cdot dm^{-3}$ stock solution of Zn(II) was prepared by dissolving 4.40 g of $ZnSO_4 \cdot 7H_2O$ into ultrapure water and then diluted to 1000 cm^3. Working solutions of Zn(II) were prepared from the stock solution by dilution with ultrapure water.

Dithizone ($C_{13}H_{12}N_4S$, Macklin) and Tween-80 ($C_{24}H_{44}O_6(C_2H_4O)_n$, Kermel) were used for Zn(II) determination. Nitric acid (HNO_3) and sodium hydroxide (NaOH) were used as regulators to adjust pH, and both of them were purchased from Sinochem, China. Ultrapure water (18.2 MΩ·cm) was generated with a Barnstead NANO Pure Diamond Water Purification System.

Characterization

Zn(II) concentrations were tested by dithizone water phase spectrophotometry method, which was modified according to *UDC 614.777:543.42:546.47*. The photometric measurements were performed at 525 nm with a model TU-1901 double-beam ultraviolet and visible spectrophotometer (UV-Vis, PERSEE, China) with ultrapure water as the reference solution.

Zeta potentials of clays were measured with a JS94H2 model microscopic electrophoresis apparatus (Powereach.com, China) and each test was repeated four times. The pH values of samples were checked by acidometer PHSJ-4A. The particle sizes of clay minerals were observed and analyzed by using the optical microscope software (ZEISS Axio Scope. A1, Germany), and d_{90} was defined as the apparent particle size relevant to 90% of cumulative distribution. Scanning electron micrographs (SEM) were obtained using a scanning electron microscope (JOEL JSM-7500F, Japan). X-ray diffractions (XRD) were obtained using a D8 Advance (Bruker) X-ray diffract meter with Cu Kα radiation (λ = 1.5418 Å). The samples were scanned at a scan rate of 0.02 s^{-1} in a 2θ range of 4–80.

Adsorption experiments

All the experiments were conducted using a batch equilibration approach at a constant temperature (25 °C). The 250 cm^3 Erlenmeyer flasks containing the clays and metal solution were shaken for a certain time in a thermostatic rotary shaker operating at 150 rpm and then centrifuged (5 min, 8000 rpm) immediately. The concentration of Zn(II) in supernatant was determined by UV-Vis. The adsorption percentage (%) Zn(II) ions

onto clay minerals and the adsorption capacity q_e (mg·g^{-1}) after equilibrium was calculated by equations as follows:

$$\text{Adsorption percentage} = \frac{C_0 - C_e}{C_0} \cdot 100 \tag{1}$$

$$q_e = \frac{(C_0 - C_e)V}{m} \tag{2}$$

where C_0 is the initial concentration of Zn(II) ions (mg·dm^{-3}), C_e is the final or equilibrium concentration (mg·dm^{-3}), V is the volume of Zn(II) solution (cm^3), and m is the weight of clay (g).

The concentration of clay was 8 g·dm^{-3} for bentonite and 100 g·dm^{-3} for kaolinite, and the initial concentration of Zn(II) ions was set as 100 mg·dm^{-3} with pH 6.0, unless other stated. Figure 1 shows the mole fraction of hydrolyzed Zn(II) species relative to total soluble metal concentration at 25 °C. It is clearly that the main species is Zn^{2+} at pH=6. The effect of solution pH on adsorption was studied by adjusting the initial solution pH from 1 to 9.

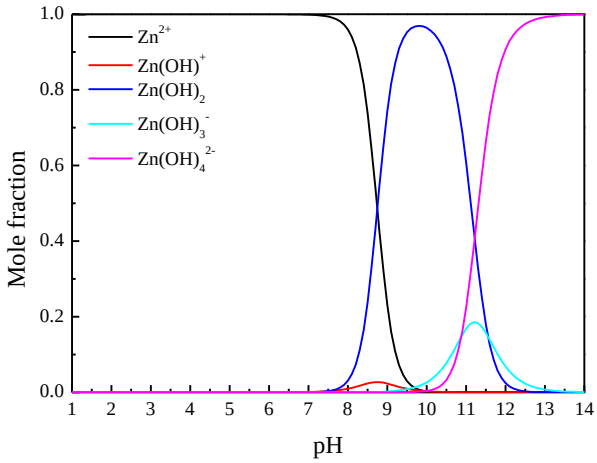

Fig. 1. Mole fraction of hydrolyzed Zn(II) species relative to total soluble metal concentration at 25 °C

The adsorption kinetics were performed by collecting samples at definite intervals time in the range of 5–90 min. The adsorption isotherms were obtained by varying the initial concentrations of Zn(II) from 100 to 600 mg·dm^{-3} at 25 °C, 35 °C and 45 °C. The thermodynamics were calculated from the temperature dependent adsorption isotherms. All the experiments were conducted in triplicate to get more accurate results. Statistical analysis was conducted with Origin pro 8.5 software.

Results and discussion

Effect of initial pH

The solution pH is an important factor, which affects the surface charge of clays and the degree of ionization and specification of Zn(II) (Gu et al., 2007; Srivastava et al., 2005). The effect of initial pH on adsorption of Zn(II) is shown in Fig. 2(a). In the lower pH range, the absorption increases rapidly with the increasing pH. However, the solution pH has a slight impact on the adsorption at the pH range of 8-9. This result lies in the formation of a Zn(II) oxyhydroxide layer coating on the clay surface decreasing Zn(II) adsorption. Therefore, the adsorption at higher pH values also involve the formation of metal complexes ($Zn(OH)^+$, $Zn(OH)_3^-$ etc.) and hydroxide precipitation ($Zn(OH)_2$).

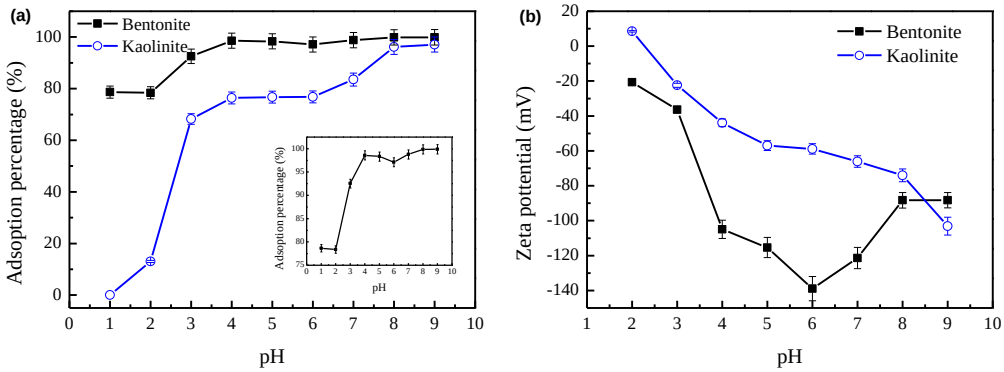

Fig. 2. Effect of pH on Zn(II) adsorption (a) and zeta potential of two clays (b)

The surface charge of clays is a function of pH and can be indicated by zeta potential, which has a great influence on the adsorption capacity of clays (Chakir et al., 2002; Niriella et al., 2006). The zeta potentials of bentonite and kaolinite are shown in Fig. 7(b). It can be seen that the zeta potential of bentonite is strongly negative and the iso-electric point (IEP) cannot be seen. In contrast, the zeta potential of kaolinite decreases with the increasing pH, and the IEP of kaolinite can be tested as pH=2.28. At lower pH (<4), the zeta potential of clays is less negative, which results in the weak electrostatic attraction between Zn(II) ions and the clay surface and ultimately leads to the poor Zn(II) adsorption at lower pH. The low adsorption is also due to the competition adsorption between hydrogen ions in solution and Zn(II) ions for the active sites on clay surfaces (Zhang et al., 2010). In addition, the more negative charge of bentonite is the reason that bentonite has a higher adsorption capacity than kaolinite over the whole pH range from 2 to 9.

Effect of contact time and adsorption kinetics

Figure 3 shows the adsorption capacity of two clays as a function of contact time. Apparently the adsorption of Zn(II) increases with time and the equilibrium is reached within 30 min for bentonite and 60 min for kaolinite. The adsorption of Zn(II) is rapid during the first 5 min and then it gradually increases slowly. The reason for this is that at the start there are abundant adsorption sites on clay minerals available for combining and Zn(II) concentration in the solution is high. As it closes to equilibrium, the adsorption sites are almost occupied by Zn(II) ions, and the surface and interlays of clay become difficult to be combined and filled in. The two stage adsorption with the first stage rapid and the second stage slow has also been reported in other literatures (El-Ashtoukhy et al., 2008; Zhang et al., 2011). It is obvious that bentonite has a higher capacity than kaolinite, and the maximum Zn(II) adsorption capacity of bentonite and kaolinite is 11.88 mg·g^{-1} and 0.87 mg·g^{-1} respectively.

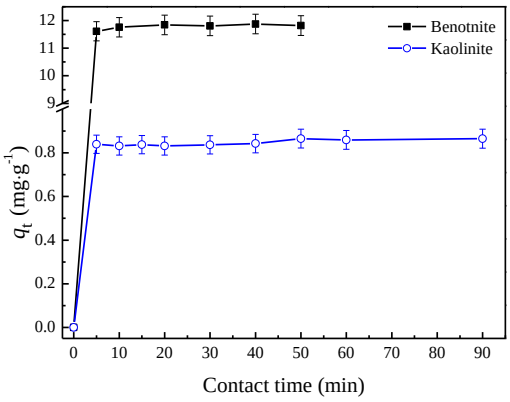

Fig. 3. Effect of contact time on Zn(II) adsorption

To inspect the rate processes of Zn(II) transporting from solution to clay-Zn(II) interface, the adsorption kinetics were tested with the following well known models: pseudo-first order and pseudo-second order were utilized. The pseudo-first order equation is:

$$q_t = q_e[1 - \exp(-k_1 t)] \tag{3}$$

where k_1 (min^{-1}) is the pseudo-first order kinetic constant, q_t (mg·g^{-1}) is the adsorption capacity at time t (Futalan et al., 2011; Gerente et al., 2007). The pseudo-second order kinetic equation is given by the linear form:

$$\frac{t}{q_t} = \frac{1}{k_2 q_e^2} + \frac{1}{q_e} \cdot t = \frac{1}{v_0} + \frac{1}{q_e} \cdot t \tag{4}$$

where k_2 (g·mg^{-1}·min^{-1}) is the pseudo-second order kinetic constant, v_0 (mg·g^{-1}·min^{-1}) is the initial adsorption rate (Gerente et al., 2007).

The kinetic data were fitted by the two kinetic models and the plots (q_e vs t) are given in Fig. 4 and the kinetic parameters are listed in Table 1. Based on the correlation coefficients (R^2), the kinetics of Zn(II) adsorption on two clays can be described well by pseudo-second order kinetic equation (R^2 > 0.999). The initial adsorption rate of bentonite (v_0, 252.53 mg·g^{-1}·min^{-1}) is much higher than that of kaolinite (1.78 mg·g^{-1}·min^{-1}), which can be attributed to the expanded lattice of bentonite (Chakir et al., 2002). However, the rate constant of bentonite (k_2, 1.80 g·mg^{-1}·min^{-1}) is lower than that of kaolinite (2.37 mg·g^{-1}·min^{-1}). This should be owing to the lower bentonite concentration, which means more competition between Zn(II) ions in binding to the fewer adsorption sites. The q_e values of bentonite (11.85 mg·g^{-1}) and kaolinite (0.87 mg·g^{-1}) show a better agreement with experimental values (11.88 and 0.87 mg·g^{-1} respectively).

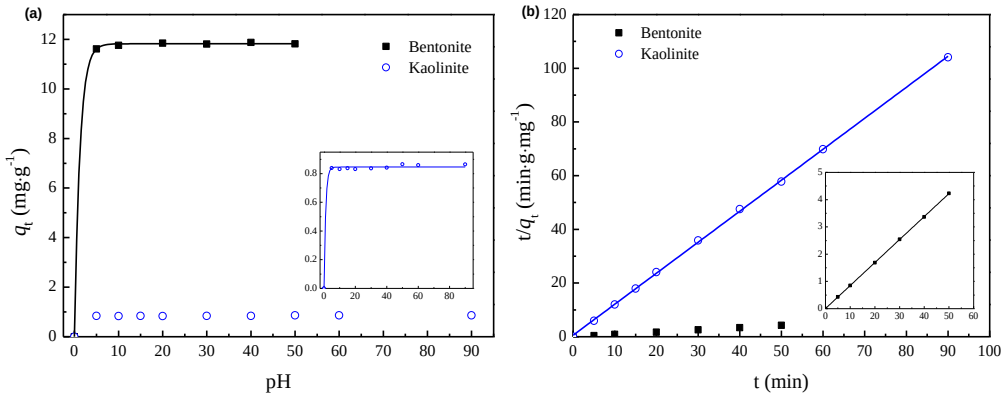

Fig. 4. Pseudo-first order plots (a) and pseudo-second order plots (b) for Zn(II) adsorption

Table 1. Kinetic parameters for adsorption of Zn(II) on two clays

Clay minerals	Pseudo-first order			Pseudo-second order			
	k_1	q_e	R^2	k_2	q_e	v_0	R^2
Bentonite	0.81	11.82	0.99993	1.80	11.85	252.53	0.99998
Kaolinite	0.95	0.85	0.99743	2.37	0.87	1.78	0.99976

Adsorption isotherms

To investigate the maximum adsorption capacity of clays for Zn(II) ions, the equilibrium concentrations of Zn(II) ions in the solid phase and in the liquid phase were modeled by common isotherms namely Langmuir isotherm and Freundlich isotherm. The Langmuir isotherm describes the monolayer adsorption and is represented as follows:

$$q_e = \frac{q_m b C_e}{1 + b C_e} \tag{5}$$

where q_m (mg·g^{-1}) is the maximum adsorption capacity, and b (dm^3·mg^{-1}) is the Langmuir constant connected with the free energy of adsorption and represents the affinity of metal ions to the binding sites on the adsorbent (Wang et al., 2008).

The Freundlich isotherm can be applied to non-ideal adsorption on heterogeneous surfaces and multilayer adsorption and it is expressed by the following equation:

$$q_e = K_f C_e^{1/n} \tag{6}$$

where K_f (mol$^{1-(1/n)}$·dm$^{3(1/n)}$·g^{-1}) and n are the Freundlich constants, which respectively indicate the relative adsorption capacity and the adsorption intensity (Blanes et al., 2011). The magnitude 1/n ranging between 0 and 1 represents the favorability of adsorption and the surface heterogeneity. If 1/n is less than unity, it indicates favorable adsorption and when its value gets closer to zero, it indicates more heterogeneous adsorbent surface.

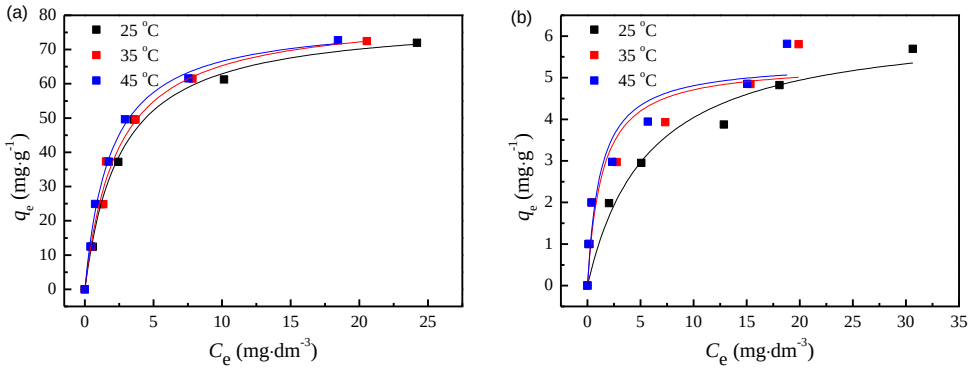

Fig. 5. Adsorption isotherms of Zn(II) on (a) bentonite and on (b) kaolinite.
Lines represent the Langmuir model simulations

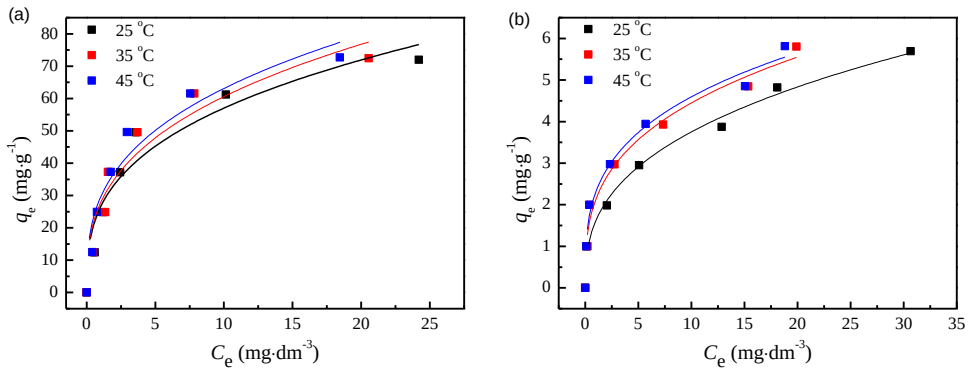

Fig. 6. Adsorption isotherms of Zn(II) on (a) bentonite and on (b) kaolinite.
Lines represent the Freundlich model simulations

The experimental data for Zn(II) equilibrium adsorption on two clays at 25, 35 and 45 ^{o}C are simulated with the Langmuir and Freundlich models. The fitting plots are illustrated in Fig. 5 and Fig. 6, and the isotherm parameters are shown in Table 2.

Table 2. Adsorption isotherm data for adsorption of Zn(II) on two clays

Clay minerals	T/^{o}C	Langmuir model			Freundlich model		
		q_m	b	R^2	K_f	n	R^2
Bentonite	25	79.20	0.39	0.9932	26.38	2.99	0.8880
	35	80.76	0.42	0.9853	27.59	2.93	0.8814
	45	79.07	0.53	0.9956	29.34	3.01	0.9050
Kaolinite	25	6.35	0.17	0.9411	1.62	2.74	0.9868
	35	5.36	0.72	0.9078	2.13	3.13	0.9687
	45	5.40	0.82	0.9150	2.31	3.35	0.9760

Comparing the correlation coefficients (R^2), the Langmuir model can best fit the adsorption data of bentonite at the given concentration range, and the Freundlich model can best fit the adsorption data of kaolinite. The parameter *n* for bentonite and kaolinite respectively varied from 2.93 to 3.01, 2.74 to 3.35, and 1/n < 1 confirms that the adsorptions of two clays for Zn(II) ions are favorable adsorption. The affinity index *b* demonstrates that the affinity between two clays and Zn(II) decreased with temperature, and bentonite has a better affinity with Zn(II) than kaolinite at 25 ^{o}C. Based on the Langmuir isotherm, the maximum adsorption of bentonite and kaolinite can be attained, ranging from 79.07 to 80.76 mg·g^{-1} and from 5.36 to 6.35 mg·g^{-1}, respectively. The Freundlich adsorption maxima of bentonite are 282-288% of the initial CEC of bentonite and 122-145% of the initial CEC of kaolinite. Metal hydroxide precipitation formed in the Zn-clay system because the adsorption capacity of Zn^{2+} surpasses the CEC of clays (Bingham et al., 1964; Udo et al., 1970). The higher q_m values of bentonite than kaolinite could be related to the more negative potential, large specific surface area and higher CEC value of bentonite than kaolinite (Alvarez-Ayuso et al., 2003).

Effect of temperature and adsorption thermodynamics

The effect of temperature on the adsorption capacity is displayed in Fig. 7.

Obviously shown in Fig.7, the adsorption capacities of bentonite and kaolinite slightly increase with the increasing temperature. This result is owing to the faster mobility and diffusion of Zn(II) ions from solution to clay-Zn(II) interface at a higher temperature. This seemingly indicates that the adsorptions of two clays for Zn(II) are endothermic processes. Actually, this needs the support of thermodynamic data.

The thermodynamic parameters for Zn(II) adsorption process, free Gibbs energy (ΔG, kJ·mol^{-1}), enthalpy (ΔH, kJ·mol^{-1}) and entropy (ΔS, kJ·K^{-1}·mol^{-1}) can be

calculated from the temperature dependent adsorption isotherms using the following equations (Bhattacharyya et al., 2011; Futalan et al., 2011):

$$\Delta G = -RT \ln K \tag{7}$$

$$\ln K = \frac{\Delta S}{R} - \frac{\Delta H}{RT} \tag{8}$$

where K is from the Langmuir and Freundlich equations (Humpola et al., 2013), R is the universal gas constant ($J \cdot mol^{-1}\ K^{-1}$), and T is the solution temperature (K). The plot of ln$K$ vs 1/T is linear with the slope and the intercept giving values of ΔH and ΔS. The results can be found in Table 3.

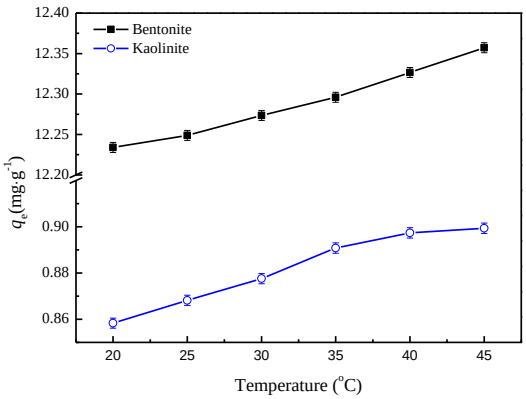

Fig. 7. Effect of system temperature on Zn(II) adsorption

Table 3. Thermodynamic data for adsorption of Zn(II) on two clays

Clay minerals	ΔH	ΔS	ΔG		
			25 °C	35 °C	45 °C
Bentonite	12.02	0.03	2.33	2.22	1.68
Kaolinite	14.13	0.05	-1.19	-1.94	-2.22

The values of ΔG for bentonite are positive, indicating that the adsorption of Zn(II) ions on bentonite is non-spontaneous at 25–45 °C and ΔG decreases from 2.33 to 1.68 $kJ \cdot mol^{-1}$ with the increasing temperature, demonstrating that the adsorption becomes less non-spontaneous. This is supported by the fact that bentonite has positive ΔH value (12.02 $kJ \cdot mol^{-1}$). It signifies that the adsorption process is endothermic and causes an increase in the entropy (ΔS = 0.03 $kJ \cdot K^{-1} \cdot mol^{-1}$). Hence increasing the temperature resulted to an increase in the Zn(II) adsorption capacity of bentonite. On the contrast, the negative ΔG for kaolinite indicates the spontaneous adsorption process, and the adsorption process of kaolinite for Zn(II) becomes more spontaneous with the temperature increasing. The adsorption process of kaolinite is also

endothermic (ΔH = 14.13 kJ·mol^{-1}) and causes an increase in the entropy (ΔS = 0.05 kJ·K^{-1}·mol^{-1}). These results demonstrate that increasing temperature is beneficial to adsorption of the two clays.

Effect of clays structural properties

In order to explore the differences of the adsorption behavior between two clays, morphological and microstructural characterizations of the samples were performed.

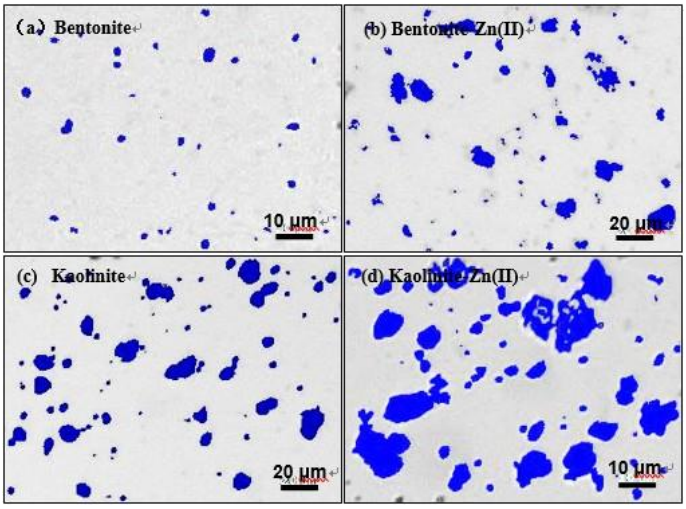

Fig. 8. The microphotographs of two clays before (a and c) and after (b and d) adsorption

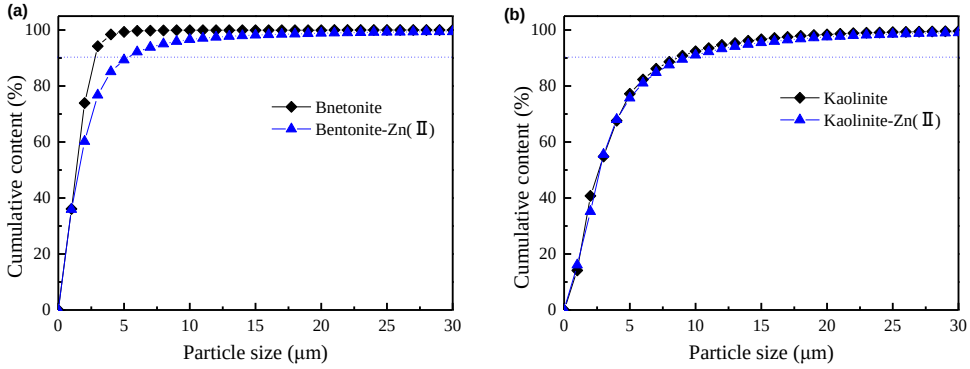

Fig. 9. Cumulative distribution of clay particle sizes before ■ and after ▲ adsorption

The microphotographs of two clays and the particle sizes before and after adsorption are shown in Figs. 8 and 9. It is obvious that the apparent particle sizes of two clays turn larger after adsorption, and d_{90} of bentonite increased from 2.79 to 5.38 μm, and kaolinite from 8.63 to 9.54 μm. The aggregation of clay particles should be attributed to the adsorption of positively charged Zn(II) ions onto the surfaces of clays

through electrostatic attraction and the negative surface of clays was partially neutralized, which reduced the repulsion of clay particles. The smaller change of kaolinite particle sizes is owing to the lower adsorption capacity.

The SEM micrographs of two clays are shown in Fig. 10.

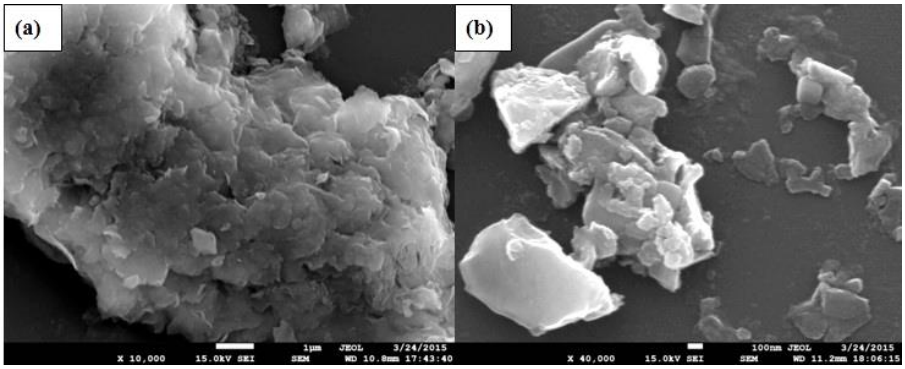

Fig. 10. SEM images of (a) bentonite and (b) kaolinite

It is obvious from Fig. 10a that, the surface of bentonite is consistent with schistose structures, which are favorable for Zn(II) adsorption. Contrastively, the kaolinite presents a relatively different surface morphology (Fig. 10b). The kaolinite particles are relatively smoother, with small fragmented and block particles adhering on the surface. These may be the reason that kaolinite has a smaller specific surface area than bentonite, which further result in the lower adsorption capacity of kaolinite.

The XRD analysis of two clays before and after adsorption of 600 $mg \cdot dm^{-3}$ Zn(II) are shown in Fig. 11. After adsorption, the basal spacing of bentonite increased from 1.4471 nm to 1.48661 nm, while that of kaolinite increased from 0.6992 to 0.71268 nm. These results indicate that Zn(II) ions were adsorbed into the interlayer by the electronic attraction (eq. 9) and aroused the increase of layer spacing. Obviously, the spacing change of bentonite is less than that of kaolinite, though bentonite has the larger layer spacing and higher adsorption capacities. These should attribute to the cation exchange reaction of Zn(II) ions with interstratified Na^+ ions of bentonite (eq. 10), and Zn(II) ions have smaller diameters (0.074 nm) than interstratified Na^+ (0.095 nm) (Nightingale Jr., 1959). Therefore, regarding to the mechanism of Zn(II) ions entering into the interlays, it can be concluded that the electronic attraction is the main adsorption mechanism for two clays, and interlayer cation exchange is another adsorption mechanism for bentonite.

$$\equiv X^- + Zn^{2+} \leftrightarrow \equiv X_3^- \cdot Zn^{2+} \tag{9}$$

$$2 \equiv X^- \cdot Na^+ + Zn^{2+} \leftrightarrow \equiv X_2^- \cdot Zn^{2+} + 2Na^+ . \tag{10}$$

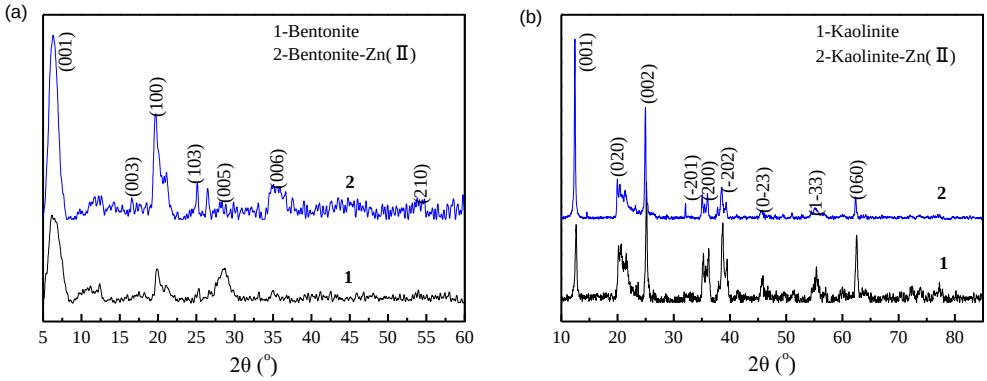

Fig. 11. The XRD patterns of bentonite (a) and kaolinite (b)

Conclusions

The adsorption behaviors of Zn(II) onto bentonite and kaolinite were investigated under various conditions. The adsorption capacities of two clays increase with the increase of contact time, solution pH and system temperature. The adsorption process that can be best described by pseudo-second order kinetic model, is governed by both electrostatic attraction and ion exchange mechanisms. The adsorption rate of two clays is much higher at the first 5 min and then turns slow afterward. Equilibrium is achieved practically in 30 min and 60 min respectively for bentonite and kaolinite. The equilibrium adsorption data of bentonite and kaolinite are fitted well by Langmuir model and Freundlich model, respectively. The adsorptions of two clays for Zn(II) are both favorable adsorption, and bentonite has a better affinity with Zn(II) than kaolinite at 25 ^{o}C. Adsorption thermodynamics indicate that the adsorptions of two clays for Zn(II) ions are both endothermic processes. The adsorption of bentonite is non-spontaneous, while that of kaolinite is spontaneous. Bentonite and kaolinite are effective adsorbents for Zn(II) ions. The adsorption percentage can reach more than 95% for 100-600 mg·dm^{-3} Zn(II) solution. Bentonite and kaolinite has potential for application in the treatment of high Zn(II)-containing lead-zinc mineral processing wastewater.

Acknowledgments

The financial supports from the National Science Fund of China (Nos. 51404213 and 51404214), the Development Fund for Outstanding Young Teachers of Zhengzhou University (No.1421324065) and the Key Research Project for Universities of Henan Province (17A450001) are gratefully acknowledged.

References

ALVAREZ-AYUSO E. and GARCIA-SANCHEZ A., 2003, *Removal of heavy metals from waste waters by natural and Na-exchanged bentonites*. Clay. Clay Miner. 51: 475-480.

APRILE F. and LORANDI R., 2012. *Evaluation of cation exchange capacity (CEC) in tropical soils using four different analytical methods*. J. Agric. Sci. 4: 278–289.

ARIAS F., SEN T.K., 2009, *Removal of zinc metal ion (Zn^{2+}) from its aqueous solution by kaolin clay mineral: A kinetic and equilibrium study*. Colloids Surf., A 348: 100-108.

BEREKET G., ARO A.Z. and OZEL M.Z., 1997, *Removal of Pb(II), Cd(II), Cu(II), and Zn(II) from Aqueous Solutions by Adsorption on Bentonite*. J. Colloid Interface Sci. 187: 338-43.

BHATTACHARYYA K.G., GUPTA S.S., 2011, *Removal of Cu(II) by natural and acid-activated clays: An insight of adsorption isotherm, kinetic and thermodynamics*. Desalination 272: 66-75.

BINGHAM F.T., PAGE A.L., SIMS J.R., 1964, *Retention of cu and zn by H-Montmorillonite*. Soil Sci. Soc. Am. J. 28: 351-354.

BLANES P., CONG C., CORTADI A., FRASCAROLI M., GATTUSO M., GARCIA S., GONZÁLEZ J., HARADA M., MATULEWICZ C., NIWA Y., PRADO H., SALA L., 2011, *Biosorption of trivalent chromium from aqueous solution by red seaweed polysiphonia nigrescens*. J. Water Resour. Prot. 03: 832-843.

CHAKIR A., BESSIERE J., KACEMI K.E., MAROUF B., 2002, *A comparative study of the removal of trivalent chromium from aqueous solutions by bentonite and expanded perlite*. J. Hazard. Mater. 95: 29-46.

CHEN J., LIU R., SUN W., QIU G., 2009, *Effect of mineral processing wastewater on flotation of sulfide minerals*. T. Nonferr. Metal. Soc. 19: 454-457.

CHEN Q., LUO Z., HILLS C., XUE G., TYRER M., 2009, *Precipitation of heavy metals from wastewater using simulated flue gas: Sequent additions of fly ash, lime and carbon dioxide*. Water Res. 43: 2605-2614.

DUKIC A.B., KUMRIĆ K.R., VUKELIC N.S., DIMITRIJEVIC M.S., BASCAREVIC Z.D., KURKO S.V., MATOVIĆ L.L., 2015, *Simultaneous removal of Pb^{2+}, Cu^{2+}, Zn^{2+} and Cd^{2+} from highly acidic solutions using mechanochemically synthesized montmorillonite-kaolinite/TiO_2 composite*. Appl. Clay Sci. 103: 20-27.

EL-ASHTOUKHY E.S.Z., AMIN N.K., ABDELWAHAB O., 2008, *Removal of lead (II) and copper (II) from aqueous solution using pomegranate peel as a new adsorbent*. Desalination 223: 162-173.

FU F., WANG Q., 2011, *Removal of heavy metal ions from wastewaters: A review*. J. Environ. Manage. 92: 407-418.

FUTALAN C.M., KAN C., DALIDA M.L., HSIEN K., PASCUA C., WAN M., 2011, *Comparative and competitive adsorption of copper, lead, and nickel using chitosan immobilized on bentonite*. Carbohyd. Polym. 83: 528-536.

GERENTE C., LEE V.K.C., CLOIREC P.L., MCKAY G., 2007, *Application of chitosan for the removal of metals from wastewaters by adsorption-mechanisms and models review*. Crit. Rev. Env. Sci. Tec. 37: 41-127.

GU X., EVANS L.J., 2007, *Modelling the adsorption of Cd(II), Cu(II), Ni(II), Pb(II), and Zn(II) onto Fithian illite*. J. Colloid Interf. Sci. 307: 317-325.

GU X., EVANS L.J., 2008, *Surface complexation modelling of Cd(II), Cu(II), Ni(II), Pb(II) and Zn(II) adsorption onto kaolinite*. Geochim. Cosmochim. Ac. 72: 267-276.

GU X., EVANS L.J., BARABASH S.J., 2010, *Modeling the adsorption of Cd (II), Cu (II), Ni (II), Pb (II) and Zn (II) onto montmorillonite*. Geochim. Cosmochim. Ac. 74: 5718-5728.

HUANG Y., HAN G., LIU J., WANG W., 2016, *A facile disposal of Bayer red mud based on selective flocculation desliming with organic humics*. J Hazard Mater, 301: 46-55.

HUANG Y., HAN G., LIU J., CHAI W., WANG W., YANG S., SU S., 2016, *A stepwise recovery of metals from hybrid cathodes of spent Li-ion batteries with leaching-flotation-precipitation process*. J Power Sources, 325: 555-564

KAYA A., OREN A.H., 2005, *Adsorption of zinc from aqueous solutions to bentonite*. J. Hazard. Mater. 125: 183-189.

HUMPOLA P.D., ODETTI H.S., FERTITTA A.E., VICENTE J.L., 2013, *Thermodynamic analysis of adsorption models of phenol in liquid phase on different activated carbons*. J. Chil. Chem. Soc. 58: 1541-1544.

JACKSON M., 1962. *Soil Chemical Analysis*. New York: Prentice-Hall Inc.

JIANG M., JIN X., LU X., CHEN Z., 2010, *Adsorption of Pb(II), Cd(II), Ni(II) and Cu(II) onto natural kaolinite clay*. Desalination 252: 33-39.

KAYA A., OREN A.H., 2005, *Adsorption of zinc from aqueous solutions to bentonite*. J. Hazard. Mater. 125: 183-189.

KUBILAY S., GURKAN R., SAVRAN A. and SAHAN T., 2007, *Removal of Cu(II), Zn(II) and Co(II) ions from aqueous solutions by adsorption onto natural bentonite*. Adsorption 13: 41-51.

LOLLINO G., GIORDAN D., THURO K., CARRANZA-TORRES C., WU F., MARINOS P., DELGADO C., YE W.M., HE Y., CHEN Y.G., CHEN B., CUI Y.J., 2015, *Adsorption, Desorption and competitive adsorption of heavy metal ions from aqueous solution onto GMZ01 bentonite*. Applied Geology for Major Engineering Projects. Springer International Publishing, 533-536.

MAVROV V., STAMENOV S., TODOROVA E., CHMIEL H., ERWE T., 2006, *New hybrid electrocoagulation membrane process for removing selenium from industrial wastewater*. Desalination 201: 290-296.

MELICHOVA Z., HROMADA L., 2013, *Adsorption of Pb^{2+} and Cu^{2+} ions from aqueous solutions on natural bentonite*. Pol. J. Environ. Stud. 22: 457-464.

MELLAH A., CHEGROUCHE S., 1997, *The removal of zinc from aqueous solutions by natural bentonite*. Water Res. 31: 621-629.

MOHAN D., CHANDER S., 2006, *Removal and recovery of metal ions from acid mine drainage using lignite-a low cost sorbent*. J. Hazard. Mater. 137: 1545-1553.

MUSSO T.B., PAROLO M.E., PETTINARI G., FRANCISCA F.M., 2014, *Cu(II) and Zn(II) adsorption capacity of three different clay liner materials*. J. Environ. Manage. 146: 50-58.

NIGHTINGALE JR., E.R., 1959, *Phenomenological theory of ion solvation. Effective radii of hydrated ions*. J. Phys. Chem. 63: 1381-1387.

NIRIELLA D. and CARNAHAN R.P., 2006, *Comparison study of zeta potential values of bentonite in salt solutions*. J. Disper. Sci. Technol. 27: 123-131.

NUÑEZ P., HANSEN H.K., AGUIRRE S., MAUREIRA C., 2011, *Electrocoagulation of arsenic using iron nanoparticles to treat copper mineral processing wastewater*. Sep. Purif. Technol. 79: 285-290.

POLAT H., ERDOGAN D., 2007, *Heavy metal removal from waste waters by ion flotation*. J. Hazard. Mater. 148: 267-273.

SEN T.K., GOMEZ D., 2011, *Adsorption of zinc (Zn^{2+}) from aqueous solution on natural bentonite*. Desalination 267: 286-294.

SHETA A.S., FALATAH A.M., AL-SEWAILEM M.S., KHALED E.M., SALLAM A.S.H., 2003, *Sorption characteristics of zinc and iron by natural zeolite and bentonite*. Micropor. Mesopor. Mat. 61: 127-136.

SINGANAN M., 2011, *Removal of lead(II) and cadmium(II) ions from wastewater using activated biocarbon*. Science Asia 37: 115-119.

SRIVASTAVA P., SINGH B., ANGOVE M., 2005, *Competitive adsorption behavior of heavy metals on kaolinite*. J. Colloid Interf. Sci. 290: 28-38.

UDO E.J., BOHN H.L., TUCKER T.C., 1970, *Zinc adsorption by calcareous soils*. Soil Sci. Soc. Am. J. 34: 405-407.

VELI S., ALYUZ B., 2007, *Adsorption of copper and zinc from aqueous solutions by using natural clay*. J. Hazard. Mater. 149: 226-233.

WANG S., PENG Y., 2010, *Natural zeolites as effective adsorbents in water and wastewater treatment*. Chem. Eng. J. 156: 11-24.

WANG S., TERDKIATBURANA T., TADE M.O., 2008, *Adsorption of Cu(II), Pb(II) and humic acid on natural zeolite tuff in single and binary systems*. Sep. Purif. Technol. 62: 64-70.

ZHANG X., LIN S., CHEN Z., MEGHARAJ M., NAIDU R., 2011, *Kaolinite-supported nanoscale zero-valent iron for removal of Pb^{2+} from aqueous solution: Reactivity, characterization and mechanism*. Water Res. 45: 3481-3488.

ZHANG X., LIN S., LU X., CHEN Z., 2010, *Removal of Pb(II) from water using synthesized kaolin supported nanoscale zero-valent iron*. Chem. Eng. J. 163: 243-248.

ZHANG X., YANG L., LI Y., LI H., WANG W., YE B., 2012, *Impacts of lead/zinc mining and smelting on the environment and human health in China*. Environ. Monit. Assess. 184: 2261-2273.